Validation of the polyyne mechanism in soot formation

T. Viola, L. Carneiro Piton, M.Idir, N. Chaumeix, A. Comandini
Institut de Combustion, Aérothermique, Réactivité et Environnement, CNRS-INSIS
Orleans, France

1 Introduction

The formation of carbonaceous soot particles is a complex mechanism involving multi-step chemical and physical processes [1-3]. Such complexity poses serious limitations and questions in the prospect of developing sufficiently accurate and reliable soot models towards cleaner combustion systems through engine design optimization and fuel reformulation. Over the years, there have been various proposals for soot formation mechanisms based on experimental results and evidence. In particular, shock tube experiments in pyrolytic conditions have been helpful to probe and validate the different mechanisms. Among these, the polyyne chemistry has been highlighted as essential for the correct prediction of experimental results from the high-temperature pyrolysis of numerous fuels [4-8]. Due to their stability at high temperatures and enhanced reactivity, the formation of polyyne affects both nucleation, through polyyne + polyyne and polyyne + PAH reactions, and particle surface growth. The basic building block for polyyne formation is acetylene, produced in large amounts in any combustion system and responsible for the HACA route [1-3], one of the main consolidated pathways for particle formation and growth. Reactions of acetylene and its radical C_2H leads to the growth of the polyyne chains, as demonstrated by the previous studies on the gas phase kinetics of acetylene pyrolysis [9,10]. Following such growth, particles can be formed. In the pioneering studies by Frenklach et al [11], the authors proposed several possible pathways to the particle gas-phase precursors, including reactions between C4 and C2 intermediates to the first-ring structures or reactions between polyacetylenes and polyacetylene radicals to form branched resonantly-stabilized intermediates. Such resonantly-stabilized intermediates can further react with other intermediates and form cyclic structures. Later models, based on the work by Krestinin [12], considered direct condensation reactions between large polyynes as responsible of soot particle nucleation. In all these models, the fast reactivity of the polyynes with the particles has been suggested. The kinetic mechanism presented in this paper combines the gas-phase chemistry of PAHs from our previous work [13] with a new phase-solid mechanism for soot, implemented with the alternative pathway of polyynes chemistry. The mechanism was validated against new experimental data as well as literature results on acetylene pyrolysis in shock tubes.

2 Experimental set-up and kinetic model

In order to evaluate an initial performance of the proposed mechanism, the key features of which are outlined below, the heated shock tube (HST) at ICARE was implemented to obtain experimental results on acetylene pyrolysis. The set-up is briefly described here. The HST has been widely used in the past

Correspondence to: andrea.comandini@cnrs-orleans.fr

for high-temperature kinetic studies, in particular on soot formation [14,15]. The HST driven section has a length of 5.15 m and a 52.4 mm diameter. It is equipped with four pressure sensors (CHIMIE METAL A25L05B) positioned along the last portion of the shock tube at a distance of 150 mm from each other. The signals from the pressure sensors are used to measure the incident shock wave velocity extrapolated to the end-wall, from which the thermodynamic conditions behind the reflected shock waves can be calculated by solving the conservation equations. The computed T_5 has a maximum error of 25-30 K due to the wave attenuation and the uncertainty in determining the exact positions of the pressure sensor sensitive surfaces. A PCB Piezotronics pressure sensor located at the end-wall of the driven section measures the pressure–time profiles. The signal acquisition is obtained with three Rohde&Schwartz RTB 2004 oscilloscopes that record pressure signals and signals from the laser detectors. Extinction measurements are performed for quantification of soot volume fractions with a He:Ne laser @ λ=633nm. The detectors are HAMAMATSU R59838 photomultiplier tubes. The soot volume fractions f_v are calculated as in equation (1), where m is the complex refractive index of soot particles, l the length crossed by the incident beam (diameter of the shock tube), λ the wavelength of the transmitted beam, I_0 the intensity of the incident beam. The function of the refractive index is assumed to be 0.36 as used in previous works in the literature, e.g. [16,17]. The experiments were performed with 0.245% and 0.35% acetylene in argon, pressure behind the reflected shock wave between 16.7 – 18.2 bar, temperatures 1750 – 1989 K and initial carbon concentrations of 3.26 – 5.38 x 10^{-17} atoms/cm3.

$$f_v = \frac{\lambda}{6\pi l \,\mathrm{Im}\left(\frac{m^2-1}{m^2+2}\right)} \ln \frac{I}{I_0} \mathrm{m} \qquad \textit{Eqn 1: Experimental evaluation of soot volume fraction } f_v.$$

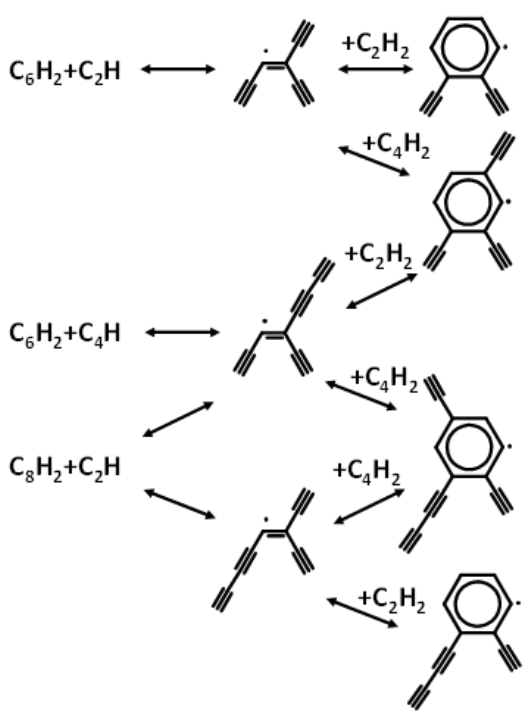

Figure 1. First ring formation from acetylene pyrolysis.

The chemical kinetic mechanism is constructed on the concept of pseudo-lumped binary carbon/hydrogen species (BINs), following the CRECK scheme [18]. Reaction rate constant parameters were adjusted according to rate rules. For aromatics chemistry, the PAH-PAHs/PAHs-BINs interactions of the molecules and radicals responsible for soot formation were developed, along with the HACA mechanism, recognized as the most influential pathway for soot formation. The reference reaction rate constant parameters for such reactions were validated against experimental results on benzene pyrolysis presented in a separate work. The chemistry of PAHs has been combined with that of the polyynes, including the fast polyacetylenic chain-attachment reactions of molecules and radicals reacting with PAHs and BINs in the inception and surface-growth. Concerning the reactions between large polyynes, the direct nucleation steps proposed by Krestinin [12] were initially tested. Despite extensive efforts in testing numerous reaction schemes and in optimizing the rate parameters in both gas-phase and solid-phase, two main challenges were encountered and could not be solved: 1) soot formation in the low temperature range of the experimental results could not be predicted implementing reasonable reference reaction rates; 2) the irreversibility of the nucleation steps to the BIN structures combined with the high stability of the polyynes at high temperatures resulted in the impossibility to model the experimentally observed drop in f_v in the high temperature ranges of the experimental datasets. For this reason, a new mechanism for PAH formation was proposed based on the suggestions by Frenklach et

al. [11]. Figure 1 shows the initiation steps for the simplest reaction systems. In particular, polyacetylene molecules and radicals can react to form branched resonantly-stabilized radical structures capable of ring-closure by further reacting with C_2H_2 and C_4H_2. These steps are reversible. The subsequent PAH growth mainly proceeds through the HACA route in analogy with the gas-phase chemistry, as well as reactions with other PAHs or polyynes. The gas-phase PAH chemistry was taken from our previous serial works on the pyrolysis of various fuel components and mixtures in single-pulse shock tube experiments. Such PAH model was coupled to the solid-phase sub-mechanisms developed in the present work. Detailed information will be presented especially for the classes involving polyynes.

3 Results and discussion

The final model includes ~ 850 species and 35,000 reactions. It can be used to predict and model soot through 0D simulations in isothermal and constant pressure batches or by evaluating constrained pressure conditions using experimental profiles in shock-tube experiments. The mechanism can be run on both Cantera [19] and Chemkin [20]. The first important validation step concerns the gas-phase reactions of acetylene and the formation of the polyyne intermediates. Compared to the original CRECK model, which is the base for the PAH model developed at ICARE, the chemistry of the polyynes was extended to larger products, up to $C_{12}H_2$. The reaction rate constant parameters were optimized based on previous literature works and validation against a variety of experimental results at different initial concentrations, temperatures, and pressures. Examples of validation results are presented in Figure 2. These include the shock tube time-history profiles from Schulz et al. [21] at nearly atmospheric pressure, temperatures above 2200 K, and acetylene mole fractions of 2% and 5% (i.e., Figure 2a), and by Kern et al. [9] at lower pressures, 3.2% acetylene, and temperatures between 2030K and 2430 K (i.e., Figure 2b). Single-pulse shock tube speciation studies on acetylene pyrolysis are also present in the literature, in particular the works by Colket [22] (3.7% C_2H_2, P ~ 8.1 bar) and by Hidaka et al. [23] (2.5-4% C_2H_2, P ~ 1.85 bar). The data by Colket [22] are shown in Figure 2c. Finally, the time-history profiles by Kern et al. [9] on diacetylene pyrolysis were also used as validation targets. Overall, the model is capable of reasonably well reproducing the majority of the experimental results on acetylene pyrolysis, providing confidence in the use of such a model as a base for testing the soot chemistry, in particular related to the polyyne mechanisms.

The experimental work on soot particle formation in the HST shock tube was performed at two initial acetylene concentrations (0.245% and 0.35%). The results were simulated, constraining the pressure time-history based on the experimental measurement for each experiment. The experimental and modeling f_v profiles are presented in Figures 3a and 3b. The simulations are scaled by a factor of 2. The simulations correctly reproduce the shape of the experimental profiles and the relative soot volume fractions at the different temperature conditions (1711 K to 1954 K for 0.35% acetylene, 1819 K to 1896 K for 0.245% acetylene). There is a slight underprediction of the data at lower initial fuel concentrations, but this could be due to larger uncertainties derived from the reduced soot quantities and consequently the small signals measured. The soot volume fractions measured at specific reaction times are reported in Figures 3c and 3d. The profiles at 0.5 ms and 1 ms are well simulated by the model within a factor of 2, especially for the data obtained with 0.35% C_2H_2. The experimental and modeling profiles were also used to extract other kinetic parameters that characterize the soot formation process, as the soot induction times (Figure 3e) and the surface growth rates (Figure 3f). The induction times are correctly simulated by the model, both in terms of global activation energies (between 29 kcal/mol and 33 kcal/mol for all sets) and absolute values, despite a slight overprediction of the induction times for the 0.245% C_2H_2 dataset. Comparison between the literature induction delay times (experiments and simulations) and the current measurements are presented in Figure 4. The induction times are normalized by multiplying them by the carbon concentrations as proposed in the literature [11]. The current measurements are in line with the general observed trend, which shows a decrease in the normalized soot induction times with a decrease in the carbon concentration from 2.5 mol/m^3 [24] to 1.1 mol/m^3 [25]. The results in the

literature extend to temperatures higher than 2000 K, the indicative limit in the present work. At these conditions, the profiles seem to have a change in slope which is not captured by the model (Figure 4b). On the other hand, the simulations well reproduce the experimental profiles below 2000 K. Concerning the surface growth rates, the model shows the absence of global activation energies, while the experimental trends provide slightly negative or positive values (-10 kcal/ mol and 3 kcal/mol). Concerning the most accurate dataset at 0.35% initial fuel concentration, the growth rates derived from the simulations are 58% lower, on average, compared to the experiments. The simulated growth rates are here multiplied by a factor of 2 as for the f_v values.

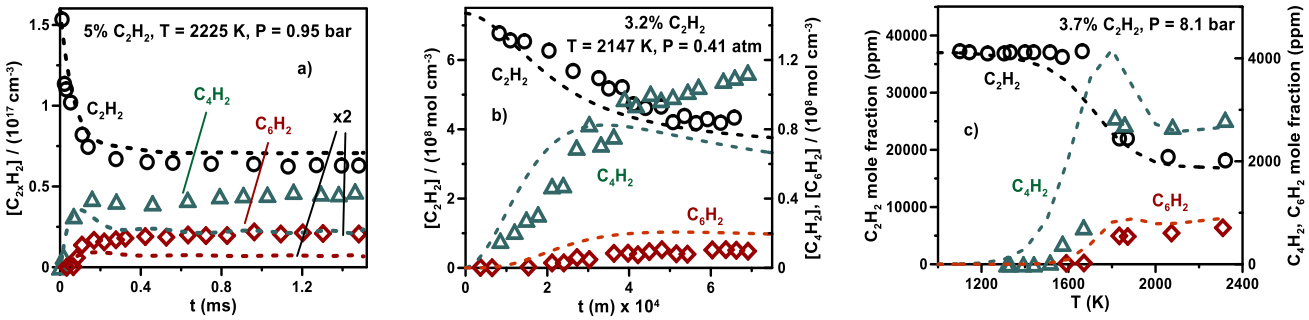

Figure 2. Gas-phase model validation.

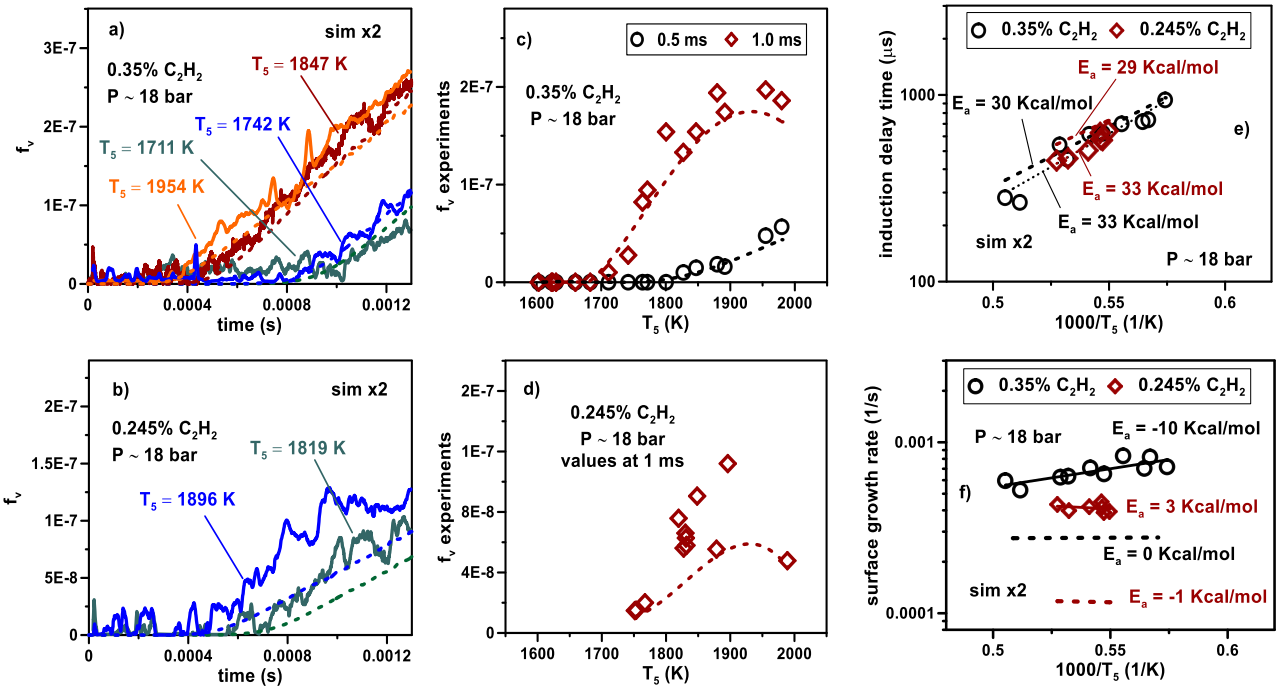

Figure 3: ICARE-HST experimental data vs simulations (dashed lines).

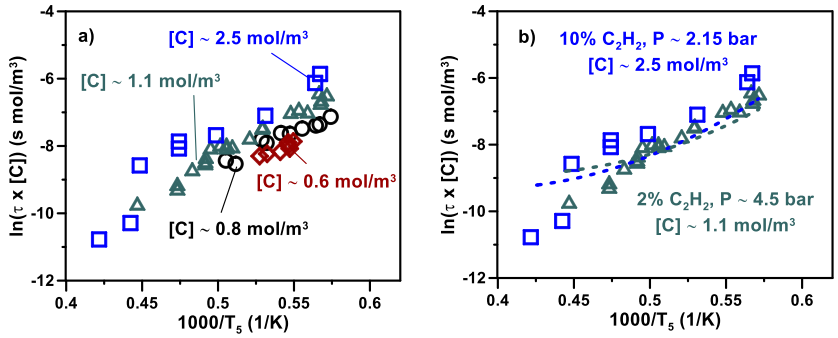

Figure 4. Comparison of literature experiments vs. HST-ICARE data and prediction of soot induction times. ◯ HST-ICARE; ▱ Drakon [24]; ∆ Eremin [25]; ◊ HST-ICARE, lines simulations.

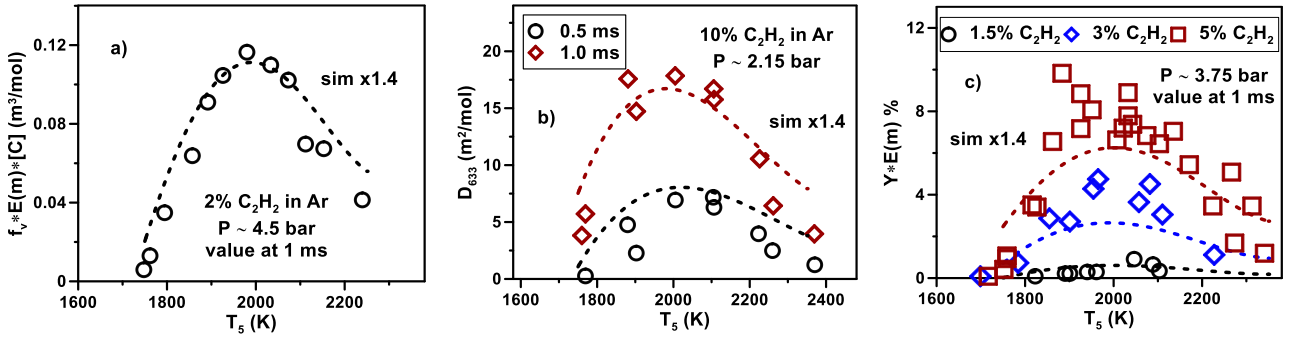

Figure 5. Soot volume fractions from shock-tube literature data under pyrolytic conditions vs current simulations (dashed line).

Comparisons were also made with other experimental f_v data from the literature at different pressure conditions and initial C_2H_2 concentrations. These include, among the others, the profile obtained at 1 ms reaction time with 2% acetylene and pressures around 4.5 bar [25] (Figure 5a), the datasets at 0.5 ms and 1 ms reaction times with 10% acetylene and pressures around 2.15 bar [24] (Figure 5b), and the profiles at 1 ms reactions time and pressures around 3.75 bar with different C_2H_2 mole fractions from 1.5% to 5% [26] (Figure 5c). The simulations are corrected by a factor of 1.4 in this case, while E(m) = 0.36 is considered for calculating the different experimental parameters starting from f_v. The model can correctly reproduce the experimental profiles over the entire temperature range and conditions.

Acknowledgements

This project has received funding from the European Research Council (ERC) under the European Union's Horizon 2020 research and innovation programme (grant agreement No. 756785).

References

[1] Bockhorn H. (1994). A Short Introduction to the Problem. In Soot Formation in Combustion-Mechanisms and Models, Bockhorn H., Ed.; Springer Series in Chemical Physics, Volume 59, pp 3-9.
[2] Lighty J. S., Veranth J. M., Sarofim A. F. 2000. Combustion aerosols: factors governing their size and composition and implications to human health. J. Air Waste Manage. 50, 1565-1618.
[3] M. Frenklach, H. Wang. (1994). Detailed Mechanism and Modeling of Soot Particle Formation, Soot Form. Combust. 165–192.
[4] Vlasov P.A., Warnatz J. (2002). Detailed kinetic modeling of soot formation in hydrocarbon pyrolysis behind shock waves

[5] Zhil'tsova I.V., Zaslonko I.S., Karasevich Yu.K., Wagner H.Gg. (2000). Nonisothermal effects in the process of soot formation in ethylene pyrolysis behind shock waves. Kinet Catal 41, 76–89.
[6]Wen J.Z., Thomson M.J., Lightstone M.F., Rogak S.N. (2006). Detailed Kinetic Modeling of Carbonaceous Nanoparticle Inception and Surface Growth during the Pyrolysis of C6H6 behind Shock Waves. Energy Fuels 20, 547–559.
[7] Naydenova I., Nullmeier M., Warnatz J., Vlasov P.A. (2004). Detailed Kinetic Modeling of Soot Formation During Shock-Tube Pyrolysis of C6h6: Direct Comparison with the Results of Time-Resolved Laser-Induced Incandescence (lii) and Cw-Laser Extinction Measurements. Combustion Science and Technology 176, 1667–1703.
[8] Eigentler F., Gerlinger P. (2022). A Detailed PAH and Soot Model for Complex Fuels in CFD Applications. Flow Turbulence Combust 109, 225–251.
[9] Wu C.H., Singh H.J., Kern R.D. (1987). Pyrolysis of acetylene behind reflected shock waves. International Journal of Chemical Kinetics 19, 975–996.
[10] Kiefer J.H., Von Drasek W.A., Von Drasek, W.A. (1990). The mechanism of the homogeneous pyrolysis of acetylene. Int J of Chemical Kinetics 22, 747–786.
[11] Frenklach M., Taki S., Durgaprasad M.B., n.d.(1983). Soot Formation in Shock-Tube Pyrolysis of Acetylene, Allene, and 1,3-Butadiene;
[12] Krestinin, A.V. (1998). Polyyne model of soot formation process. Symposium (International) on Combustion, Twenty-Seventh Sysposium (International) on Combustion Volume One 27, 1557–1563.
[13] Hamadi A., Sivaramakrishnan R., Cano Ardila F.E., Tranter R.S., Abid S., Chaumeix N., Comandini, A., (2024). Styrene thermal decomposition and its reaction with acetylene under shock tube pyrolysis conditions: An experimental and kinetic modeling study. Proceedings of the Combustion Institute 40, 105481.
[14] De Iuliis S., Chaumeix N., Idir M., Paillard C.-E. (2008). Scattering/extinction measurements of soot formation in a shock tube. Experimental Thermal and Fluid Science, Fifth mediterranean combustion symposium 32, 1354–1362.
[15] Mathieu O., Djebaïli-Chaumeix N., Paillard C.-E., Douce F. (2009). Experimental study of soot formation from a diesel fuel surrogate in a shock tube. Combustion and Flame 156, 1576–1586.
[16] Agafonov G. L., Bilera I. V., Vlasov P. A., Kolbanovskii Y. A., Smirnov V. N., Tereza, A. M. (2015). Soot formation during the pyrolysis and oxidation of acetylene and ethylene in shock waves. Kinet. Catal. 56, 12-30.
[17] Nativel D., Herzler J., Krzywdziak S., Peukert S., Fikri M., Schulz C. (2022). Shock-tube study of the influence of oxygenated additives on benzene pyrolysis: Measurement of optical densities, soot inception times and comparison with simulations. Combust. Flame, 111985.
[18] Nobili A., Cuoci A., Pejpichestakul W., Pelucchi M., Cavallotti C., Faravelli T. (2022). Modeling soot particles as stable radicals: a chemical kinetic study on formation and oxidation. Part I. Soot formation in ethylene laminar premixed and counterflow diffusion flames. Combustion and Flame 112073.
[19] Cantera is an open-source suite of tools for problems involving chemical kinetics, thermodynamics, and transport processes. https://cantera.org/;
[20] https://www.ansys.com/fr-fr/products/fluids/ansys-chemkin-pro;
[21] Aghsaee M., Dürrstein S.H., Herzler J., Böhm H., Fikri M., Schulz C. (2014). Influence of molecular hydrogen on acetylene pyrolysis: Experiment and modeling. Combustion and Flame 161, 2263–2269.
[22] Colket M.B. (1988). The pyrolysis of acetylene and vinylacetylene in a single-pulse shock tube. Symposium (International) on Combustion, Twenty-First Symposuim (International on Combustion) 21, 851–864.
[23] Hidaka Y., Hattori K., Okuno T., Inami K., Abe T., Koike T., n.d. (2000) Shock-Tube and Modeling Study of Acetylene Pyrolysis and Oxidation.
[24] Drakon A., Eremin A., Mikheyeva E., Shu B., Fikri M., Schulz C. (2018). Soot formation in shock-wave-induced pyrolysis of acetylene and benzene with H2, O2, and CH4 addition. Combustion and Flame 198, 158–168.
[25] Eremin A., Mikheyeva, E., Selyakov I. (2018). Influence of methane addition on soot formation in pyrolysis of acetylene. Combustion and Flame 193, 83–91.
[26] Agafonov G.L., Bilera I.V., Vlasov P.A., Kolbanovskii Y.A., Smirnov V.N., Tereza A.M. (2015). Soot formation during the pyrolysis and oxidation of acetylene and ethylene in shock waves. Kinet Catal 56, 12–30.